

Thioredoxin interacting protein (Txnip) deficiency disrupts the fasting-feeding metabolic transition¹

Sonal S. Sheth,^{*} Lawrence W. Castellani,^{*} Soumya Chari,^{*} Cory Wagg,[‡] Christopher K. Thippavong,^{*} Jackie S. Bodnar,^{*} Peter Tontonoz,[#] Alan D. Attie,⁺ Gary D. Lopaschuk,[‡] and Aldons J. Lusis^{*,§}

^{*} Departments of Human Genetics, Medicine, Molecular Biology Institute, and Microbiology, Immunology, & Molecular Genetics, University of California Los Angeles, 47-123 CHS, David Geffen School of Medicine at UCLA, Los Angeles, California 90095 USA.

[‡] 423 Heritage Medical Research Building, Faculty of Medicine and Dentistry, University of Alberta, Edmonton, Alberta, Canada T6G 2S2.

[#] Molecular Biology Institute, Howard Hughes Medical Institute, Department of Pathology and Laboratory Medicine, University of California, Los Angeles, California 90095 USA.

⁺ Department of Biochemistry, University of Wisconsin-Madison, Madison, Wisconsin 53706 USA.

[§]To whom correspondence should be addressed:

Aldons J. Lusis
David Geffen School of Medicine at UCLA
47-123 Center for Health Sciences
Los Angeles, CA 90095-1679
Phone: (310) 825-1359
Fax: (310) 794-7345
jlusis@mednet.ucla.edu

Running Title: The Metabolic Consequences of Txnip Deficiency

¹ The abbreviations used are: Txnip, thioredoxin interacting protein; Vdup1, vitamin D₃ up-regulated protein; Txn, thioredoxin; TCA, tricarboxylic citric acid; SREBP-1c, sterol-response element binding protein-1c; PPAR- γ , peroxisome proliferator-activated receptor- γ ; PGC-1 α , PPAR- γ coactivator-1 α ; FFA, free fatty acids; LDL, low density lipoprotein; VLDL, very low density lipoprotein; PEPCK, phosphoenolpyruvate carboxykinase; G6Pase, glucose-6-phosphatase; GK, glucokinase; FAS, fatty acid synthase; MCAD, medium chain acyl CoA dehydrogenase; SCD1, stearoyl CoA desaturase 1; AOX, acyl CoA oxidase; Glut2, glucose transporter 2; Glut4, glucose transporter 4; TNF α , tumor necrosis factor α ; FCHL, familial combined hyperlipidemia; CREB, cAMP response element binding protein; p-CREB, phosphorylated CREB.

Abstract

Through a positional cloning approach, the thioredoxin interacting protein gene (*Txnip*) was recently identified as causal for a form of combined hyperlipidemia in mice (1). We now show that *Txnip* deficient mice in the fed state exhibit an altered response to nutrition, including elevated levels of plasma ketone bodies and free fatty acids, decreased glucose, and increased hepatic expression of PPAR- γ Coactivator-1 α (PGC-1 α), phosphoenolpyruvate carboxykinase (PEPCK), glucose-6-phosphatase (G6Pase), and acyl CoA oxidase (AOX). Dramatic differences in the expression of key metabolic enzymes were also observed in other tissues, and the fat to muscle ratio of *Txnip* deficient mice was increased by about 40%. We demonstrate an effect of *Txnip* on the redox status, as the *Txnip* deficient mice in the fed state had a significant increase in the ratio of NADH:NAD⁺. Surprisingly, we observed that *Txnip* deficient mice and wild-type mice had similar levels of thioredoxin activity, suggesting that the effects of *Txnip* deficiency may be mediated in part by other interactions. These results indicate a role for *Txnip* in the metabolic response to feeding and the maintenance of the redox status.

Supplementary key words

Redox status; nutritional status; hypoglycemia; hypertriglyceridemia; fatty acid oxidation; mice

Introduction

We previously identified a naturally occurring mouse model for familial combined hyperlipidemia (FCHL), a disorder characterized by elevated plasma cholesterol and triglycerides (2). Subsequently, positional cloning showed that the hyperlipidemia resulted from a spontaneous nonsense mutation in the gene for thioredoxin-interacting protein (*Txnip*), also known as vitamin D₃ up-regulated protein 1 (*Vdup1*) (1). *Txnip* was originally identified in a yeast two-hybrid screen for proteins that bind to thioredoxin (Txn), a thiol-oxidoreductase that undergoes NADPH-dependent reduction and has multiple roles in intracellular signaling and resistance to oxidative stress (3-6). The nonsense mutation in the hyperlipidemic mouse resulted in dramatically reduced mRNA levels and a truncated *Txnip* peptide lacking the region of the C-terminus required for Txn binding (1). We showed that *Txnip* deficient mice exhibited increased production of triglyceride-rich lipoproteins and ketone bodies. Liver slices isolated from *Txnip* deficient mice also exhibited reduced hepatic CO₂ production, suggesting an impairment of the tricarboxylic acid (TCA) cycle. We proposed that the *Txnip* deficiency reduced flux through the TCA cycle, sparing fatty acids for incorporation into triglycerides and ketone bodies (1). Since the only known function of *Txnip* was binding to and inhibiting Txn, we speculated that the *Txnip* deficient mice would exhibit increased Txn activity and an imbalance of the cellular redox state, perhaps resulting in elevated NADH levels which could lead to the down-regulation of the TCA cycle (1).

Subsequently, Donnelly *et al.* (7) used stable isotope methods to demonstrate that *Txnip* deficient mice exhibit increased lipogenesis and increased hepatic triglyceride and cholesterol ester stores. Recently, Hui *et al.* (8) reported that fasted *Txnip* deficient mice had depressed glucose levels and that the ablation of pancreatic β cells by treatment with streptozotocin reduced

The Metabolic Consequences of Txnip Deficiency

the hypertriglyceridemia phenotype, suggesting that increased insulin secretion may be a primary contributing factor to the metabolic alterations. They also presented evidence that the hypertriglyceridemia resulted in part from elevated expression of the lipogenic transcription factor, sterol-response element binding protein-1c (SREBP-1c) (8). Schulze *et al.* (9) presented evidence that the oxidative stress contributing to the complications of diabetes may be mediated in part by the induction of Txnip by elevated glucose.

We now report metabolic studies of Txnip deficient mice in the fed and fasted states. We observed profound alterations in both lipid and glucose metabolism in multiple tissues despite the absence of significant differences in insulin levels, suggesting direct metabolic effects of Txnip in liver, heart, and adipose. In several respects, the metabolic profile of fed Txnip deficient mice resembles that of mice subjected to prolonged fasting. One regulatory factor that appears to be involved is the transcriptional coactivator, PGC-1 α , whose expression is significantly elevated in the Txnip deficient mice in the fed state. We have also examined mechanisms mediating the effects of Txnip deficiency. We observed a significant elevation of NADH in fed Txnip deficient mice, consistent with an effect on the redox status, but, surprisingly, the activity of Txn was not significantly increased. Our results indicate that Txnip is required for appropriate metabolic responses to feeding.

Experimental Procedures

Animal husbandry and diets

The development of the recombinant congenic mutant mouse strain HcB-19/*Dem*, and recombinant inbred strains, and congenic strains were described previously(1, 2, 10). To study the effects of the *Txnip* mutation on various backgrounds, all mice were housed under conditions meeting the guidelines of the Association for Assessment and Accreditation of Laboratory Animal Care and were housed in groups of five or less animals per cage and maintained on a 12 hour light-dark cycle at an ambient temperature of 23°C. They were allowed *ad libitum* access to water and rodent chow containing 6% fat (Diet No. 8604, Harlan Teklad, Madison, Wis). For the studies conducted in the fasted state, samples were obtained at approximately 1200 h after an overnight fast. All animal care and experimental protocols were approved by the UCLA Animal Research Committee.

Body Composition

Fat to muscle mass ratio was determined using nuclear magnetic resonance (NMR) spectroscopy. The NMR instrument (Bruker Biospin, Billerica, MA) was calibrated according to manufacturer's instructions. To measure body composition, Txnip deficient and wild-type mice were individually contained in a cylinder and placed in the instrument. The amount of total body mass was determined as the sum of fat mass, lean mass, and water.

Plasma lipid, ketone body, lactate, glucose, insulin, and leptin determinations

Mice were either fed *ad libitum* or fasted for 18 hours prior to retro-orbital bleeding, and were bled under isofluorane anesthesia using EDTA as the anticoagulant. Plasma lipids were

The Metabolic Consequences of Txnip Deficiency

determined as described previously (11). In order to minimize the hydrolysis of triglycerides, the blood samples are immediately placed on ice, centrifuged to separate the plasma, and frozen. To validate the FFA assay, we also measured free glycerol from the triglycerides between the two strains. There was no significant difference in glycerol levels indicating that the increased FFA in Txnip deficient mice is not due to *in vitro* hydrolysis. Levels of the ketone body β -hydroxybutyrate were determined in duplicate using a kit (#310-A, Sigma). Blood collection tubes were pre-chilled on ice and the samples centrifuged within 5 minutes to remove erythrocytes in order to obtain accurate plasma lactate concentrations, which were measured in duplicate using a lactate kit (#735-10, Sigma). Plasma glucose concentrations were measured in triplicate using a glucose kit (#315-100, Sigma). For glucose measurements, blood collection tubes were pre-chilled on ice and the samples centrifuged within 5 minutes in order to minimize glucose metabolism by erythrocytes. Plasma insulin levels were determined in duplicate by sensitive rat insulin RIA (SRI-13K, LINCO Diagnostics) and ELISA (#008-10-1150-01, ALPCO Diagnostics). Plasma leptin levels were measured in duplicate using a mouse ELISA kit (#MOB00, R&D Systems).

Hepatic glycogen levels

Liver tissue samples were homogenized in ddH₂O. Aliquots of the homogenate were transferred to an acetate buffer solution containing 5×10^{-5} g α -glucosidase (Sigma, cat #A7420) and 2.7 μ l α -amylase (Sigma, cat #A4268) per ml of buffer solution. Aliquots of homogenates were also transferred to acetate buffer solution containing no enzymes, to serve as a sample blank. A standard curve was generated with a serial dilution of glucose. After addition to the buffer solution the tubes were incubated at 37° C for 10 minutes, centrifuged in a microcentrifuge for 5

The Metabolic Consequences of Txnip Deficiency

min at 3000 rpm and 170 μ l of the supernatant, in triplicate, was transferred to a 96 well plate and read at 490 nm is a Molecular Devices Spectramax plus microplate reader.

Glucose and fatty acid oxidation in the heart

The University of Alberta Health Sciences Laboratory Animal Services and Welfare Committee approved all animal procedures and conformed to the guidelines of the Canadian council on Animal Care. Experiments were done as previously described (12). Txnip deficient and wild-type mice (25-30g) were heparinized (100U i.p.) 10 minutes prior to anesthetizing with 50 μ l i.p. sodium pentobarbital. The heart was quickly removed and submerged in ice-cold Krebs-Henseleit (KH) solution (118mM NaCl, 4.7mM KCl, 1.2mM KH₂PO₄, 1.2mM MgSO₄7H₂O, 2.5mM CaCl₂2H₂O, and ddH₂O). The mouse heart was cannulated in two stages: 1) the lungs were removed and the aorta was cannulated on a modified 20 gauge catheter syringe, following with a retro grade perfusion was initiated with 37°C KH solution at a 60mmHg hydrostatic pressure. The aorta was sutured to the cannula and the heart was observed for a pulse before performing the next stage, 2) the catheter and heart was removed from the injection port and moved to the main cannula. Here the remaining excess tissue was removed and the left atrium was cannulated and sutured. Following this the Langendorff line was clamped and the hearts were perfused at a 11mmHg left atrial preload and a 50mmHg aortic afterload. The working KH solution contained, 5mM glucose, 25mM NaHCO₃, 3% fatty acid free bovine serum albumin (BSA) (Equitech-Bio Inc.), 1.2mM palmitate bound to the BSA, 100 μ U/ml human biosynthetic insulin (Novo Nordisk Inc.), [U-¹⁴C] glucose and [9,10-³H(N)] palmitate. Hyamine Hydroxide (1M)(Curtiss Laboratories Inc.) was used to capture the ¹⁴CO₂ produced by the heart, as described. The hearts were perfused 30 min aerobically. Buffer (5ml) and hyamine (2x300 μ l)

The Metabolic Consequences of Txnip Deficiency

samples were removed every 10 minutes. At the end of the protocol the ventricle was isolated, cut down and instantly frozen in liquid N₂. The remaining atria was taken down, dried and used for total dry weight of the heart. Glucose oxidation was determined by the quantitative collection of ¹⁴CO₂ produced from D-[U-¹⁴C] glucose (Amersham Biosciences). At every sample time 5 ml of buffer were taken and 2ml were used for the collection of ¹⁴CO₂ and the remaining 3 ml of buffer were placed under paraffin oil and used for the ³H₂O extraction assay. Palmitate oxidation was measured quantitatively from [9, 10-³H] palmitate acid (Perkin Elmer) from the collection of ³H₂O. Duplicate, capped 7ml scintillation vials containing 500ul of H₂O to which 1.5ml capless microfuge tubes containing 200ul of buffer sample were incubated at 50°C for 24 hr then removed and cooled at 4°C overnight. A standard of [³H] water (Sigma) was also prepared to find the percentage of ³H₂O transferred in the heating and cooling process. The capless microfuge tubes were disposed and the scintillation vials were filled with 5ml of Ecolite (ICN) scintillant and measured for activity.

Fatty acid oxidation in the soleus muscle

Following an 18 hour fast, C3H/DiSnA (WT) and Txnip deficient mice were anesthetized with pentobarbital (50mg/kg body wt) and the soleus muscle was isolated under a dissecting microscope. The muscles were weighed and immediately incubated for 40 min in Krebs-Henseleit buffer under 95% O₂:5% CO₂, that contained 5.5 mM glucose, 3% BSA, 1 mM palmitate and [¹⁴C-U]-palmitic acid (2.5μCi/ml). Rates of fatty acid oxidation were assessed by determining radioactivity in ¹⁴CO₂ trapped in hyamine hydrochloride as described previously(13).

The Metabolic Consequences of Txnip Deficiency

RNA analysis

Mice were either fed *ad libitum* or fasted for 18 hours and were sacrificed by cervical dislocation. Total RNA was isolated from liver, gonadal fat pads, and skeletal muscle with TriZol reagent according to the manufacturer's instructions (Invitrogen). For reverse transcription (RT)-PCR analysis, first-strand cDNAs were synthesized with the use of 1 µg total RNA isolated from the liver, gonadal fat pads, and skeletal muscle and by use of Taqman RT Reagents (ABI). Taqman real-time quantitative PCR experiments were done using Applied Biosystems 7700 sequence detector as previously described (14). Results are presented as averages of duplicates normalized to 36B4 expression.

Western blot analyses

Mice were either fed *ad libitum* or fasted for 18 hours and were sacrificed by cervical dislocation. Liver tissue was immediately removed and placed in liquid nitrogen. Frozen tissue was weighed and added to a lysis buffer (20mM HEPES, 100mM KCl, 300mM NaCl, 10mM EDTA, 0.1% Nonidet P-40, and a cocktail of protease inhibitors (Roche)). For Western blot analysis, appropriate protein samples were reduced in dithiothreitol (DTT), boiled, electrophoresed on 10% SDS-PAGE gels, and electroblotted onto ECL nitrocellulose membranes by using a transfer apparatus from Invitrogen according to manufacturer's instructions. Membranes were blocked with phosphate-buffered saline with 0.1% Tween20/5% nonfat dry milk overnight, washed, and incubated with primary and secondary antibodies for 2 hours and 1 hour, respectively. The primary antibodies for thioredoxin (Santa Cruz Biotechnologies) and p-CREB (Upstate) are commercially available antibodies. The secondary antibody used was horseradish peroxidase-conjugated anti-rabbit IgG for thioredoxin and p-CREB (Amersham).

The Metabolic Consequences of Txnip Deficiency

Primary and secondary antibodies for thioredoxin were used at 1:500 and 1:1000 dilutions, respectively. For p-CREB, primary and secondary antibodies were used at 1:350 and 1:1000 dilutions, respectively. The membranes were washed extensively with Phosphate-buffered saline/0.1% Tween20 after primary and secondary antibody incubation and detected by using the ECL Western blotting kit (Amersham) according to the manufacturer's suggested protocol. Protein levels for Txn and p-CREB were normalized against β -actin and α -tubulin protein levels, respectively, to ensure equal loading. To generate an antibody against Txnip, several approaches yielded poor results. First, synthetic peptides against three different immunogenic regions of the protein were created, however, all were non-specific. We then attempted to use a bacterial expression vector system to generate Txnip protein, but the protein appeared to be toxic to various strains of bacteria. We also were able, through the generous contributions of the Lee and Yodoi laboratories (9, 15), to obtain polyclonal antibodies against mouse and human Txnip. Unfortunately, in our hands, these also yielded non-specific results.

Nucleotide determinations

Pyrimidine dinucleotide levels were determined as described elsewhere with slight modifications (16). Due to the lack of availability of C3H/DiSnA mice, C3H/HeJ mice were used as wild-type mice for these experiments. To ensure that the lipid profiles were similar, we measured the triglycerides in the C3H/HeJ mice used in the experiment. The average fasted triglyceride value in C3H/HeJ was 72.2 mg/dl, and the average triglyceride value in C3H/DiSnA was 68.8 mg/dl. Mice were either fed *ad libitum* or fasted for 18 hours and were sacrificed by cervical dislocation. Liver tissue was immediately removed and freeze-clamped in liquid nitrogen. 75 mg of frozen tissue was homogenized in the 750 μ l extraction buffer (0.2 M potassium cyanide, 0.06

The Metabolic Consequences of Txnip Deficiency

M potassium hydroxide, 1 mM bathophenanthrolinedisulfonic acid). Homogenate was extracted with chloroform and centrifuged for 6 minutes at 13,000 rpm. The supernatant was once again extracted with chloroform and centrifuged. The aqueous sample was filtered through a 0.45 μm positively charged nylon-55 filter. The sample was then diluted with 4 parts mobile phase (0.2 M ammonium sulfate, 4 mM tetrabutylammonium hydrogen sulfate, pH 6) and immediately placed on the HPLC machine. HPLC analysis used a Supelcosil LC-18-T column (Supelco) with a guard column. The HPLC program was as follows: after 1 minute at 96% mobile phase and 4% methanol, the methanol increases at 0.8%/minute for 25 minutes. The column was then flushed with water for 12 minutes, pure methanol for 18 minutes, and then water for another 12 minutes before returning to starting conditions. The flow rate was 1 ml/min, the fluorescence is detected at an excitation wavelength of 330 nm and emission wavelength of 460 nm.

Insulin reducing assay for Txn activity

The insulin disulfide reduction assay was essentially performed as described elsewhere with slight modifications (17). Liver protein was isolated as described above. 20 μg of protein was preincubated at 37°C for 20 min with 2 μl of DTT activation buffer (50 mM HEPES (pH 7.6), 1 mM EDTA, 1 mg/ml BSA, and 2 mM DTT) for a total volume of 10 μl . 40 μl of reaction mixture, containing 200 μl of 1 M HEPES (pH 7.6), 40 μl of 0.2 M EDTA, 40 μl of NADPH (40 mg/ml), and 500 μl of insulin (10 mg/ml) was added. The reaction began with the addition of 10 μl of rat Txn reductase (100 A412 U/ml) (Sigma), and the incubation continued for 20 min at 37°C. The reaction was terminated with 0.5 ml of 6 M guanidine-HCl and 1 mM DTNB (3-carboxy-4-nitrophenyl disulfide), and the absorbance at 412 nm was measured. To control for

The Metabolic Consequences of Txnip Deficiency

other oxidoreductases, samples were treated with and without Txn Reductase. Rat Txn (Sigma) was used as to generate a standard curve ranging from 100-1200 ng/ml.

Statistical analyses

Data are presented as mean \pm SEM, with n indicating the number of mice. The statistical significance of differences in plasma lipid levels, glucose and fatty acid oxidation, gene expression levels, protein and activity levels, and ratios between reduced and oxidized pyrimidine nucleotides between the 2 groups was determined with ANOVA. Differences were considered statistically significant at $P<0.05$.

Results

General characteristics of Txnip deficient mice.

We have now examined the Txnip deficient mice on a variety of genetic backgrounds, including C3H/DiSnA, C57BL/10ScSnA, C57BL/6J, BALB/c, and CAST/Ei, and all exhibited similarly elevated plasma triglyceride and ketone body levels. The experiments reported here were performed on mice with a C3H/DiSnA genetic background between 3 and 5 months of age. Txnip deficient mice were similar in weight and activity to wild-type or heterozygous littermates with no differences in food consumption (data not shown). The litter sizes of the Txnip deficient mice were reduced, and in crosses involving heterozygous mice, lower than expected frequencies of Txnip deficient mice were born (data not shown). We have also noted that some older Txnip deficient mice, approximately 9 months of age or older, develop liver adenomas and carcinomas (Sheth S.S., Ghazalpour A., Bodnar J.S., Lusis A.J., unpublished).

Although Txnip deficient mice are similar in weight to wild-type littermates, the proportion of fat to muscle mass is significantly different between the two groups. Using nuclear magnetic resonance (NMR) analysis, the fat to muscle mass ratio was 1.4 times higher in Txnip deficient mice than wild-type mice (fig. 1a). This was primarily due to a significant decrease in the muscle mass, which was confirmed by directly measuring the soleus muscle mass in Txnip deficient mice (fig. 1b).

Txnip deficient mice exhibit an abnormal metabolic profile in the fed and fasted states.

In order to define the metabolic profile of the Txnip deficient mice, we measured various lipid and glucose metabolic parameters in the fed and fasted states. Although normally increased in the fasted state, the Txnip deficient mice exhibited elevated levels of plasma ketone bodies,

The Metabolic Consequences of Txnip Deficiency

with an approximate 2-fold increase compared to wild-type in the fed state and six-fold increase occurring in the fasted state (fig. 1c). Plasma free fatty acid (FFA) levels, which if altered, should be elevated in the fasted state due to increased adipose tissue triglyceride lipolysis, were significantly elevated in both the fed and fasted states in Txnip deficient mice (fig. 1d). Likewise, plasma glucose levels were reduced in both the fed and fasted states, the decrease being particularly prominent (53%) in the fasted state (fig. 1e). Glycogen, which is metabolized in the fasted state, was also reduced in livers of the Txnip deficient mice in the fasted state (fig. 1f). Thus, several metabolic alterations associated with fasting, including increased ketone bodies, increased FFA, and decreased glucose levels, were all observed in Txnip deficient mice in the fed state (Fig. 1).

Under normal physiologic conditions, there is a decrease in the plasma triglyceride levels in the fasted state. However, the Txnip deficient mice exhibited the opposite response, an increase in plasma triglycerides (fig. 1g). We previously also showed that Txnip deficient mice exhibit decreased flux through the TCA cycle in liver as judged by the production of CO₂ (1), which would spare fatty acids for incorporation into triglycerides. As discussed below, fatty acid synthase expression was also elevated in Txnip deficient mice. Plasma LDL and VLDL cholesterol levels were also higher in fasted Txnip deficient mice (fig. 1h).

Since there are clearly important metabolic interactions between liver, muscle, and adipose, it is likely that the decreased muscle mass contributes to the metabolic perturbations observed in livers of Txnip deficient mice. Notably, the decreased muscle mass would influence glucose and triglyceride utilization. Interestingly, despite the decreased muscle mass, plasma lactate levels were increased. Plasma lactate levels were significantly higher, by approximately 55%, in the fed state of the Txnip deficient mice (fig. 1i). The elevated plasma lactate, which

represents the muscle equivalent of ketone bodies, may be explained in part by a decrease in pyruvate oxidation due to elevated fatty acids, resulting in pyruvate being redirected to lactate.

Plasma leptin levels were measured in the fed and fasted states. In Txnip deficient mice, the levels appeared to be elevated in both the fed and fasted states, although the results did not reach statistical significance with a p value of 0.22 and 0.23, respectively. In the fed state, the average leptin level in Txnip deficient mice was 7.1 ng/ml in comparison to the wild-type which had 4.7 ng/ml. In the fasted state, the Txnip deficient had an average leptin level of 3.4 ng/ml, and the wild-type had an average leptin level of 1.8 ng/ml. Increased plasma leptin would stimulate the esterification of fatty acids to be incorporated into triglycerides, which could explain the hypertriglyceridemia observed in Txnip deficient mice.

Txnip influences glucose and fatty acid oxidation in the heart and skeletal muscle.

As previously reported (1), Txnip is widely expressed, with high levels of mRNA in heart and muscle. Therefore, glucose and fatty acid oxidation were measured in isolated perfused heart, and fatty acid oxidation was measured in isolated soleus muscles. In the Txnip deficient heart, glucose oxidation, as measured by the release of CO₂ from the oxidation of ¹⁴C-labeled glucose, was substantially decreased (fig. 1j). Rates of fatty acid oxidation were determined by measuring the amount of ³H₂O released from the oxidation of ³H-labeled palmitate in the heart and ¹⁴CO₂ released from the oxidation of ¹⁴C-labeled palmitate in the soleus muscle. There was no significant difference in fatty acid oxidation in the heart between the wild-type and Txnip deficient mice (fig. 1k). In wild-type hearts, fatty acid oxidation provided 64% of the acetyl CoA for the TCA cycle while in Txnip deficient mouse hearts, 82% of the acetyl CoA for the TCA cycle originated from fatty acids. The contribution of glucose oxidation and fatty acid

The Metabolic Consequences of Txnip Deficiency

oxidation to TCA cycle activity in the isolated working hearts was calculated using the following values: 2 moles of acetyl CoA supplied to the TCA cycle from every mole of glucose oxidized and 8 moles of acetyl CoA supplied to the TCA cycle from every mole of palmitate oxidized. This indicates that the Txnip deficient heart is preferentially utilizing fatty acids as a substrate over glucose.

We also measured fatty acid utilization in the soleus muscle in the fasted state by determining CO₂ release using ¹⁴C-labeled palmitate as the substrate. Fatty acid oxidation was increased 35% in the Txnip deficient soleus muscle in the fasted state (fig. 11). According to the Randle hypothesis, increased plasma FFA could explain the increased fatty acid uptake in the muscle (18, 19).

Txnip deficiency alters the expression of PGC-1 α and its downstream targets.

In order to understand the molecular basis of the above metabolic perturbations resulting from the *Txnip* mutation, real-time quantitative PCR was used to analyze the expression of metabolic candidate genes in the liver, adipose, and skeletal muscle in the fed and fasted states. PGC-1, regulator of genes involved in gluconeogenesis, ketogenesis, and fatty acid oxidation, is induced in response to fasting (20). Txnip deficient mice in the fed state showed a 5-fold increase in PGC-1 α expression in comparison to the wild-type mice in the fed state (fig. 2a). When subjected to fasting, wild-type mice exhibited an increase in PGC-1 α expression, whereas in Txnip deficient mice, PGC-1 α expression was unchanged but still slightly elevated compared to wild-type mice (fig. 2a).

Consistent with the known effects of PGC-1 α on gluconeogenic genes (20), phosphoenolpyruvate carboxykinase (PEPCK) and glucose-6-phosphatase (G6Pase) were

The Metabolic Consequences of Txnip Deficiency

increased 10-fold and 3-fold, respectively, in the fed Txnip deficient livers (fig. 2b,c). Whereas PEPCCK and G6Pase were induced in the fasted state of the wild-type mice, in the Txnip deficient mice, the expression was unchanged or reduced relative to the fed state (fig. 2b,c). The fasting hepatic expression of glucokinase (GK), which catalyzes the first step in glycolysis, was higher in Txnip deficient mice, whereas wild-type mice exhibited a decrease in expression upon fasting (fig. 2d). Thus, the fact that Txnip deficient mice exhibit a dysregulation in response to feeding can be explained in part by the altered expression of PGC-1 α .

It has been shown that PGC-1 α is regulated by insulin, glucocorticoids, and cAMP response element binding protein (CREB) (21). The entire family of thioredoxin proteins activate CREB, with the highest activation occurring through the action of nucleoredoxin and glutaredoxin (22). Txnip binds to a conserved cysteine consensus sequence found in the thioredoxin family, so it would seem feasible that Txnip could bind to other members. To determine whether the increase in PGC-1 α in the fed state is the result of increased activation of CREB, we measured the protein levels of phosphorylated CREB (p-CREB) between Txnip deficient and wild-type mice. We observed no significant difference in protein levels of p-CREB between Txnip deficient and wild-type livers in the fed state (fig. 2e). This suggests that the difference in PGC-1 α expression may be occurring through an alternative mechanism.

Effects of Txnip deficiency on hepatic fatty acid metabolic enzymes.

We previously showed that Txnip deficient mice secrete more triglycerides from the liver, resulting in elevated plasma levels of VLDL-cholesterol, VLDL-triglycerides, and both apolipoprotein B-100 and B-48 (2). To test whether this is due to increased fatty acid synthesis, we measured the expression of fatty acid synthase (FAS) in liver using real-time PCR. Although

The Metabolic Consequences of Txnip Deficiency

FAS expression was suppressed during fasting, in Txnip deficient mice, FAS expression was elevated as compared to wild-type mice in both fed and fasting conditions (fig. 3a). Since plasma triglycerides in Txnip deficient mice are elevated only during fasting (fig. 1g), there are presumably other, compensatory changes during the fed state. One such change involves medium chain acyl CoA dehydrogenase (MCAD), which is involved mitochondrial β -oxidation. In the fasted state, livers of Txnip deficient mice have decreased CO₂ production from fatty acids, increased ketone body production, and increased triglyceride production (1). The Txnip deficient mice appeared to have increased expression of MCAD in both the fed and fasted states, although the levels did not reach statistical significance (fig. 3b). Consistent with previous studies that show an increase in the activity of SCD1 in fasted Txnip deficient mice, we observed an increase in the fed and fasted levels of SCD1 mRNA (fig. 3c) (23). It has been shown that SCD1 is a key regulator in determining the fate of fatty acids in the liver (24). Our results showing increased expression of SCD1 are consistent with this concept.

We also measured acyl-CoA oxidase (AOX), an enzyme that catalyzes the first step of peroxisomal fatty acid oxidation and is an important target that is upregulated during fasting (25). In wild-type mice, AOX expression was increased during fasting (fig. 3d). In Txnip deficient mice, the enzyme level was already 10-fold elevated in the fed state compared to wild-type (fig. 3d). Thus, again, the profile of Txnip deficient mice appears similar to that of a fasted animal.

Regulation of glucose metabolism by Txnip.

The decrease in glucose levels during fasting (Fig. 1) suggests that there may be dysregulation of insulin production or responsiveness, and Hui *et al.* (8) observed significant

differences in insulin levels between Txnip deficient and wild-type mice in the fasted state. We measured insulin levels in several groups of mice in both fed and fasted states using two different assay procedures, an ELISA (fig. 4a) and a radioimmunoassay (data not shown). Although there was a trend towards increased levels of insulin in both fed and fasted states, the differences were not statistically significant (fig. 4a). The more modest elevation in insulin levels may be due to the difference of the age of the mice used in the previous study (6 months) in comparison to the mice used in this study (3-5 months) (8). To examine whether alterations in glucose metabolism resulted from altered expression of glucose transporters, we measured the expression of Glut2 in liver and Glut4 in muscle. No significant differences in either transporter were observed in the fed and fasted states (fig. 4b,c). The expression of Glut4 was also unchanged in white adipose tissue (see below).

Tissue-specific dysregulation of genes in adipose tissue and skeletal muscle of Txnip deficient mice.

PGC-1 α is important in adipose tissue metabolism. For example, it is induced in response to cold and regulates adaptive thermogenesis in brown adipose tissue (26). We examined PGC-1 α mRNA expression in white adipose tissue from the gonadal fat pads. In the fed state, Txnip deficient mice had decreased levels of PGC-1 α mRNA as compared to wild-type mice, and unlike wild-type mice, PGC-1 α mRNA levels did not decrease upon fasting (fig. 5a).

The effect of Txnip deficiency on adipose metabolism was further examined by measuring mRNA levels of FAS and Glut4. In the fed state, the levels of FAS in adipose were substantially decreased in Txnip deficient mice. The gene expression patterns of PGC-1 α and FAS in the Txnip deficient adipose tissue are significantly different than those seen in the liver.

The Metabolic Consequences of Txnip Deficiency

While PGC-1 α mRNA levels in the Txnip deficient adipose tissue increase in the fasted state, the levels remain constitutively high between the fed and fasted states in the Txnip deficient liver. FAS mRNA expression patterns were also significantly different between the Txnip deficient adipose tissue and liver. Regardless of whether the Txnip deficient mice were fed or fasted, the FAS levels in the adipose tissue were extremely low. However, in the Txnip deficient liver, the FAS levels increased upon fasting. This indicates that the Txnip deficiency has tissue specific effects, and it specifically has opposing effects on the adipose tissue and the liver. In contrast to PGC-1 α and FAS expression, mRNA levels of glucose transporter, Glut4, in adipose tissue were unchanged between wild-type and Txnip deficient mice (fig. 5b,c).

One characteristic response of adipose tissue to fasting is an increased expression of tumor necrosis factor α (TNF α), which is involved in the stimulation of lipolysis (27). In Txnip deficient mice, TNF α levels were higher in the fed state (10-fold), but not significantly different from the wild-type in the fasted state (fig. 5d). Thus, in adipose tissue, as well as liver, fed Txnip deficient mice exhibited an abnormal response to nutritional signals.

We also examined the expression of PGC-1 α and AOX in the white skeletal muscle. PGC-1 α expression in white muscles of the leg was not significantly affected by Txnip deficiency under fed or fasted conditions (fig. 5e). AOX levels in Txnip deficient mice were decreased in the fed state and were not significantly different in the fasted state (fig. 5f). Because AOX is primarily involved in peroxisomal fatty acid oxidation, the unchanged level of AOX in the fasted Txnip deficient mice is not inconsistent with the observed increase in palmitate oxidation in the soleus muscle.

Redox status of Txnip deficient mice.

We previously proposed that Txnip deficiency would result in elevated levels of reduced pyrimidine nucleotides and that this would result in inhibition of flux through the TCA cycle, thereby sparing fatty acids for incorporation into triglycerides (1). To test this hypothesis, we quantitated the levels of these reduced and oxidized pyrimidine nucleotides, utilizing a high performance liquid chromatography (HPLC) assay (16). Figure 6 shows the chromatograms and ratios between the pyrimidine nucleotides in the Txnip deficient and wild-type mice. In the fed state, Txnip deficient mice had a 2-fold increase in the ratio of NADH:NAD⁺ although there were no statistically significant differences observed between Txnip deficient and wild-type mice in the fasted state (fig. 6c,d). The peaks for NADP⁺ were too small given our background to reliably estimate the NADPH:NADP⁺ ratio (Fig. 6). While these data are consistent with our observation that Txnip deficient mice show a metabolic dysregulation in the fed state, the change in NADH:NAD⁺ ratio does not appear to be able to explain the metabolic perturbations of Txnip deficiency in the fasted state.

Thioredoxin may not mediate the effects of the Txnip deficiency.

In vitro studies suggest that Txnip acts as a negative regulator of thioredoxin activity and protein levels (15). In cells transfected with *Txnip*, thioredoxin activity was reduced by 50%. However, after upregulating *Txnip* 9-fold upon 1, 25-dihydroxyvitamin D₃ treatment in HL-60 cells, there was only a modest decrease in thioredoxin activity (15). Since the critical binding region of Txnip is absent in our mutant mice, and Txnip mRNA is greatly reduced, we expected that our mice would exhibit enhanced expression and activity of thioredoxin *in vivo*. We measured the hepatic protein levels of thioredoxin in the fed and fasted states. The activity of

The Metabolic Consequences of Txnip Deficiency

thioredoxin was also measured in the fed and fasted liver by detecting the amount of reduced insulin in an enzymatic assay as previously described (17). Surprisingly, the protein level (fig. 7a) and activity of thioredoxin (fig. 7b) were not discernibly different between Txnip deficient mice and wild-type mice in both the fed and fasted states. These data suggest that the metabolic perturbations in Txnip deficient mice may involve other interactions as well.

Discussion

We previously used positional cloning to identify *Txnip* as the gene underlying hypertriglyceridemia in a naturally occurring mouse model (1). We have now examined in detail the metabolic perturbations resulting from Txnip deficiency. Several conclusions have emerged from these studies. First, Txnip deficiency results in a disruption in the fasting-feeding metabolic transition, perturbing glucose as well as lipid metabolism in a variety of tissues. Second, the deficiency is associated with large alterations in the expression of key metabolic enzymes and regulators, including altered expression of PGC-1 α in liver and adipose. Third, there is an altered redox status in the livers of the Txnip deficient mice, which may be the cause or the result of the metabolic abnormalities observed in the Txnip deficient mice. Further, the fact that Txn activity was not significantly affected raises the possibility of other interactions.

The normal response to prolonged fasting is increased lipolysis of adipose triglycerides, release of fatty acids into the circulation, and uptake of fatty acid by liver and other tissues, where they can be oxidized. During fasting, the liver exhibits increased gluconeogenesis and increased production of ketone bodies, which can be utilized by the brain, skeletal muscle, cardiac muscle and other tissues as a source of energy. Plasma levels of glucose and triglycerides normally decrease in a fasted state. In the fed state, Txnip deficient mice exhibit many of the characteristics of a fasted state, including elevated ketone bodies, decreased glucose levels, and elevated plasma FFA (Fig. 1). The lower hepatic glycogen levels seen the fasted Txnip deficient mice can be explained in part by a trend ($p=.07$) towards lower glycogen in the fed state. Since the Txnip deficient mice already have a depleted source of glycogen in the fed state, the fasted levels are much lower. The higher plasma leptin levels in the Txnip deficient mice are consistent with the increased expression of SCD1 in the liver. Ntambi *et al.* (24) have

The Metabolic Consequences of Txnip Deficiency

shown that SCD1 deficiency leads to increased fatty acid oxidation and decreased triglyceride synthesis along with decreased leptin levels. The increased expression and activity of SCD1 in fasted Txnip deficient mice suggests that the Txnip deficiency may control the fate of fatty acids in the liver through SCD1 (23). The lack of a significant difference in MCAD mRNA expression levels also suggests that the dysregulation leading to increased ketone body production and decreased CO₂ production in the Txnip deficient livers occurs downstream of β -oxidation. The adipose tissue of fed Txnip deficient mice also exhibited characteristics of a fasted state; in particular, the Txnip deficient mice had dramatically (10-fold) increased expression of TNF α in the fed state (fig. 5d). In the Txnip deficient adipose tissue, the expression levels of metabolic genes, such as PGC-1 α and FAS, were significantly different from levels observed in the Txnip deficient liver, indicating a tissue specific effect.

One of the fundamental regulatory molecules involved in response to fasting is PGC-1 α . This transcriptional coactivator is involved in nutritional and other environmental responses in liver, muscle, and adipose (20, 28, 29). Whereas PGC-1 α is normally induced in liver in response to fasting, Txnip deficient mice in the fed state had PGC-1 α levels exceeding those of fasted wild-type mice (fig. 2a). Furthermore, the known downstream targets of PGC-1 α , such as PEPCK and G6Pase, also exhibited similar changes in expression levels (fig 2b, c).

Several recent studies have identified Txnip as a potential key regulator of glucose homeostasis. Thus, *Txnip* expression is dramatically upregulated in isolated pancreatic β cells upon exposure to glucose (30). In rat fibroblasts treated with glucose, *Txnip* induction occurs even in the presence of cyclohexamide, implying that *Txnip* is a glucose-responsive immediate early gene (31). Recent studies showed that streptozotocin treatment of Txnip deficient mice reduced the hypertriglyceridemia phenotype in the fasted state, implying that the effects of Txnip

The Metabolic Consequences of Txnip Deficiency

are mediated in part by insulin levels (8). Hui *et al.* (8) supported this conclusion by showing that, in the fasted state, insulin levels were elevated in Txnip deficient mice and that the level of insulin-inducible transcription factor, SREBP-1c, was elevated in fasted Txnip deficient mice. In our present study, we observed a trend toward increased insulin levels in both fed and fasted states (fig. 4a), but these were not statistically significant, which could be explained, in part, by the difference in ages of the animals used in this study and the larger sample size. To test for possible methodological problems, we utilized two different assays, radioimmunoassay (data not shown) and ELISA. Recently, Schulze *et al.* (9) presented evidence that the oxidative stress contributing to the complications of diabetes may result in part from the induction of Txnip by elevated glucose.

Our studies and two other recent studies agree in finding that the hyperlipidemic phenotype of Txnip deficient mice is due, at least in part, to increased triglyceride synthesis, resulting from elevated expression of fatty acid synthase. This is probably mediated in large part by increased expression of the key lipogenic transcription factor, SREBP-1c (8). The mechanism leading to the reduced glucose levels in fasted Txnip deficient mice will require additional biochemical and kinetic studies. Our studies do not provide evidence of decreased hepatic glucose synthesis or increased glucose utilization by peripheral tissues, which would account for lower glucose. One possible explanation, supported by increased plasma lactate levels in the fed state, is increased Cori cycling.

The cellular redox state is critical for maintaining homeostasis, and we have now demonstrated that Txnip influences the levels of NADH. This is likely to have a broad metabolic impact. For example, reduced pyrimidine nucleotides promote, whereas oxidized pyrimidine nucleotides inhibit, binding of transcription factors for genes involved in the circadian clock

(32). Also, there is evidence that an increased NADH:NAD⁺ ratio promotes the conversion of pyruvate to lactate (33) and that NADP⁺ inhibits gluconeogenesis (34). Consistent with this, our results show an increase in plasma lactate and hepatic gluconeogenic enzymes in the fed state of Txnip deficient mice. However, the altered redox state does not explain the changes seen in fasted Txnip deficient mice since there were no significant changes in the ratios of reduced to oxidized pyrimidine in the fasted state. It is noteworthy that hepatic ratios of reduced:oxidized glutathione were increased 30% in Txnip deficient mice in the fasted state (8).

Our data suggest the Txnip deficiency alters the metabolism in various tissues. However, our results suggest that the effects are not mediated entirely by Txn, since we failed to observe significant changes in Txn levels or in Txn activity in Txnip deficient mice. We hypothesize that Txnip may interact with other members of the Txn family, including glutaredoxin and nucleoredoxin, all of which have the “-CXXC-” motif by which Txnip is thought to interact with Txn(22, 35). Recently, Yodoi and colleagues (36) utilized a yeast two hybrid screen to identify additional proteins that interact with Txnip. Among these is importin α 1, which facilitates the transport of Txnip into the nucleus (36). It is clear that the nonsense mutation of *Txnip* we have studied here would not interact with Txn. In studies with truncated Txnip, it has been shown that amino acids 134-395 of Txnip were required for Txn binding and inhibition of activity (35). Since the nonsense mutation of *Txnip* occurs at amino acid 97 (1), the critical binding region of Txnip is absent. Moreover, due to nonsense-mediated RNA decay, the mRNA levels of the mutant *Txnip* transcript were greatly decreased (1).

In conclusion, our results indicate that the normal changes in glucose and fatty acid metabolism in response to feeding is dependent upon *Txnip* expression. The mechanism appears to be mediated in part by effects on the redox status of cells, but precisely how redox status

The Metabolic Consequences of Txnip Deficiency

affects key transcription factors and enzymes involved in the metabolism of lipids and glucose is unclear. It is also possible that the altered redox status is a consequence rather than a cause of some these metabolic perturbations.

Acknowledgments

This study was supported by NIH grant HL28481 (AJL), HL30568 (PT), and Canadian Institutes of Health Research (GDL). Soumya Chari was supported in part by NIH training grant T32-HL069766.

References

1. Bodnar, J. S., A. Chatterjee, L. W. Castellani, D. A. Ross, J. Ohmen, J. Cavalcoli, C. Wu, K. M. Dains, J. Catanese, M. Chu, S. S. Sheth, K. Charugundla, P. Demant, D. B. West, P. de Jong and A. J. Lusis. 2002. Positional cloning of the combined hyperlipidemia gene *Hyplip1*. *Nat Genet.* **30**: 110-116.
2. Castellani, L. W., A. Weinreb, J. Bodnar, A. M. Goto, M. Doolittle, M. Mehrabian, P. Demant and A. J. Lusis. 1998. Mapping a gene for combined hyperlipidaemia in a mutant mouse strain. *Nat Genet.* **18**: 374-377.
3. Gasdaska, J. R., M. Berggren and G. Powis. 1995. Cell growth stimulation by the redox protein thioredoxin occurs by a novel helper mechanism. *Cell Growth Differ.* **6**: 1643-1650.
4. Hirota, K., M. Matsui, S. Iwata, A. Nishiyama, K. Mori and J. Yodoi. 1997. AP-1 transcriptional activity is regulated by a direct association between thioredoxin and Ref-1. *Proc Natl Acad Sci U S A.* **94**: 3633-3638.
5. Nakamura, H., K. Nakamura and J. Yodoi. 1997. Redox regulation of cellular activation. *Annu Rev Immunol.* **15**: 351-369.
6. Ueda, S., H. Nakamura, H. Masutani, T. Sasada, S. Yonehara, A. Takabayashi, Y. Yamaoka and J. Yodoi. 1998. Redox regulation of caspase-3(-like) protease activity: regulatory roles of thioredoxin and cytochrome c. *J Immunol.* **161**: 6689-6695.
7. Donnelly, K. L., M. R. Margosian, S. S. Sheth, A. J. Lusis and E. J. Parks. 2004. Increased lipogenesis and fatty acid reesterification contribute to hepatic triacylglycerol stores in hyperlipidemic *Txnip*^{-/-} mice. *J Nutr.* **134**: 1475-1480.
8. Hui, T. Y., S. S. Sheth, J. M. Diffley, D. W. Potter, A. J. Lusis, A. D. Attie and R. A. Davis. 2004. Mice lacking thioredoxin-interacting protein provide evidence linking cellular redox state to appropriate response to nutritional signals. *J Biol Chem.* **279**: 24387-24393.
9. Schulze, P. C., J. Yoshioka, T. Takahashi, Z. He, G. L. King and R. T. Lee. 2004. Hyperglycemia promotes oxidative stress through inhibition of thioredoxin function by thioredoxin-interacting protein. *J Biol Chem.* **279**: 30369-30374.
10. Demant, P. and A. A. Hart. 1986. Recombinant congenic strains--a new tool for analyzing genetic traits determined by more than one gene. *Immunogenetics.* **24**: 416-422.
11. Hedrick, C. C., L. W. Castellani, C. H. Warden, D. L. Puppione and A. J. Lusis. 1993. Influence of mouse apolipoprotein A-II on plasma lipoproteins in transgenic mice. *J Biol Chem.* **268**: 20676-20682.

12. Campbell, F. M., R. Kozak, A. Wagner, J. Y. Altarejos, J. R. Dyck, D. D. Belke, D. L. Severson, D. P. Kelly and G. D. Lopaschuk. 2002. A role for peroxisome proliferator-activated receptor alpha (PPARalpha) in the control of cardiac malonyl-CoA levels: reduced fatty acid oxidation rates and increased glucose oxidation rates in the hearts of mice lacking PPARalpha are associated with higher concentrations of malonyl-CoA and reduced expression of malonyl-CoA decarboxylase. *J Biol Chem.* **277**: 4098-4103.
13. Olubadewo, J., D. W. Morgan and M. Heimberg. 1983. Effects of triiodothyronine on biosynthesis and secretion of triglyceride by livers perfused in vitro with [3H]oleate and [14C]glycerol. *J Biol Chem.* **258**: 938-945.
14. Laffitte, B. A., S. B. Joseph, R. Walczak, L. Pei, D. C. Wilpitz, J. L. Collins and P. Tontonoz. 2001. Autoregulation of the human liver X receptor alpha promoter. *Mol Cell Biol.* **21**: 7558-7568.
15. Nishiyama, A., M. Matsui, S. Iwata, K. Hirota, H. Masutani, H. Nakamura, Y. Takagi, H. Sono, Y. Gon and J. Yodoi. 1999. Identification of thioredoxin-binding protein-2/vitamin D(3) up-regulated protein 1 as a negative regulator of thioredoxin function and expression. *J Biol Chem.* **274**: 21645-21650.
16. Adams, J. D., Jr., Klaidman, L.K. 2002. Oxidative stress and nicotinamide effects on brain pyrimidine nucleotides. *Recent Research and Development in Analytical Biochemistry.* **2**: 249-264.
17. Holmgren, A. and M. Bjornstedt. 1995. Thioredoxin and thioredoxin reductase. *Methods Enzymol.* **252**: 199-208.
18. Randle, P. J., P. B. Garland, C. N. Hales and E. A. Newsholme. 1963. The glucose fatty-acid cycle. Its role in insulin sensitivity and the metabolic disturbances of diabetes mellitus. *Lancet.* **1**: 785-789.
19. Jequier, E. 1998. Effect of lipid oxidation on glucose utilization in humans. *Am J Clin Nutr.* **67**: 527S-530S.
20. Yoon, J. C., P. Puigserver, G. Chen, J. Donovan, Z. Wu, J. Rhee, G. Adelmant, J. Stafford, C. R. Kahn, D. K. Granner, C. B. Newgard and B. M. Spiegelman. 2001. Control of hepatic gluconeogenesis through the transcriptional coactivator PGC-1. *Nature.* **413**: 131-138.
21. Herzig, S., F. Long, U. S. Jhala, S. Hedrick, R. Quinn, A. Bauer, D. Rudolph, G. Schutz, C. Yoon, P. Puigserver, B. Spiegelman and M. Montminy. 2001. CREB regulates hepatic gluconeogenesis through the coactivator PGC-1. *Nature.* **413**: 179-183.
22. Hirota, K., M. Matsui, M. Murata, Y. Takashima, F. S. Cheng, T. Itoh, K. Fukuda and J. Yodoi. 2000. Nucleoredoxin, glutaredoxin, and thioredoxin differentially regulate NF-kappaB, AP-1, and CREB activation in HEK293 cells. *Biochem Biophys Res Commun.* **274**: 177-182.

23. Attie, A. D., R. M. Krauss, M. P. Gray-Keller, A. Brownlie, M. Miyazaki, J. J. Kastelein, A. J. Lusis, A. F. Stalenhoef, J. P. Stoehr, M. R. Hayden and J. M. Ntambi. 2002. Relationship between stearoyl-CoA desaturase activity and plasma triglycerides in human and mouse hypertriglyceridemia. *J Lipid Res.* **43**: 1899-1907.
24. Ntambi, J. M., M. Miyazaki, J. P. Stoehr, H. Lan, C. M. Kendziorski, B. S. Yandell, Y. Song, P. Cohen, J. M. Friedman and A. D. Attie. 2002. Loss of stearoyl-CoA desaturase-1 function protects mice against adiposity. *Proc Natl Acad Sci U S A.* **99**: 11482-11486.
25. Hashimoto, T., W. S. Cook, C. Qi, A. V. Yeldandi, J. K. Reddy and M. S. Rao. 2000. Defect in peroxisome proliferator-activated receptor alpha-inducible fatty acid oxidation determines the severity of hepatic steatosis in response to fasting. *J Biol Chem.* **275**: 28918-28928.
26. Puigserver, P., Z. Wu, C. W. Park, R. Graves, M. Wright and B. M. Spiegelman. 1998. A cold-inducible coactivator of nuclear receptors linked to adaptive thermogenesis. *Cell.* **92**: 829-839.
27. Green, A., J. M. Rumberger, C. A. Stuart and M. S. Ruhoff. 2004. Stimulation of lipolysis by tumor necrosis factor-alpha in 3T3-L1 adipocytes is glucose dependent: implications for long-term regulation of lipolysis. *Diabetes.* **53**: 74-81.
28. Rhee, J., Y. Inoue, J. C. Yoon, P. Puigserver, M. Fan, F. J. Gonzalez and B. M. Spiegelman. 2003. Regulation of hepatic fasting response by PPARgamma coactivator-1alpha (PGC-1): requirement for hepatocyte nuclear factor 4alpha in gluconeogenesis. *Proc Natl Acad Sci U S A.* **100**: 4012-4017.
29. Puigserver, P. and B. M. Spiegelman. 2003. Peroxisome proliferator-activated receptor-gamma coactivator 1 alpha (PGC-1 alpha): transcriptional coactivator and metabolic regulator. *Endocr Rev.* **24**: 78-90.
30. Shalev, A., C. A. Pise-Masison, M. Radonovich, S. C. Hoffmann, B. Hirshberg, J. N. Brady and D. M. Harlan. 2002. Oligonucleotide microarray analysis of intact human pancreatic islets: identification of glucose-responsive genes and a highly regulated TGFbeta signaling pathway. *Endocrinology.* **143**: 3695-3698.
31. Hirota, T., T. Okano, K. Kokame, H. Shirovani-Ikejima, T. Miyata and Y. Fukada. 2002. Glucose down-regulates Per1 and Per2 mRNA levels and induces circadian gene expression in cultured Rat-1 fibroblasts. *J Biol Chem.* **277**: 44244-44251.
32. Rutter, J., M. Reick, L. C. Wu and S. L. McKnight. 2001. Regulation of clock and NPAS2 DNA binding by the redox state of NAD cofactors. *Science.* **293**: 510-514.
33. Ferraz, M., K. Brunaldi, C. E. Oliveira and R. B. Bazotte. 1997. Hepatic glucose production from L-alanine is absent in perfused liver of diabetic rats. *Res Commun Mol Pathol Pharmacol.* **95**: 147-155.

The Metabolic Consequences of Txnip Deficiency

34. Fulgencio, J. P., C. Kohl, J. Girard and J. P. Pegorier. 1996. Troglitazone inhibits fatty acid oxidation and esterification, and gluconeogenesis in isolated hepatocytes from starved rats. *Diabetes*. **45**: 1556-1562.
35. Junn, E., S. H. Han, J. Y. Im, Y. Yang, E. W. Cho, H. D. Um, D. K. Kim, K. W. Lee, P. L. Han, S. G. Rhee and I. Choi. 2000. Vitamin D3 up-regulated protein 1 mediates oxidative stress via suppressing the thioredoxin function. *J Immunol*. **164**: 6287-6295.
36. Nishinaka, Y., H. Masutani, S. I. Oka, Y. Matsuo, Y. Yamaguchi, K. Nishio, Y. Ishii and J. Yodoi. 2004. Importin alpha 1 (Rch1) mediates nuclear translocation of thioredoxin-binding protein-2 (TBP-2/VDUP1). *J Biol Chem*.

Figure Legends

Figure 1. In the fed state, Txnip deficient mice exhibit an abnormal metabolic response to nutrition. C3H/DiSnA were used as wild-type (WT) mice, indicated by solid bars, and Txnip deficient (*Txnip*^{-/-}) mice, indicated by shaded bars, were fed a chow diet and water *ad libitum*. Blood and tissue samples were collected in the fed or fasted (18 hour) state. For plasma lipid, glucose, and lactate levels, measurements are in mg/dl. (A) Ratio of fat to lean muscle mass in the fed state by NMR spectroscopy. (B) Muscle mass (g) in the fed state as determined by NMR spectroscopy. (C) Ketone bodies measured as β -hydroxybutyrate (β -HB) levels. (D) Plasma free fatty acid (FFA) levels. (E) Plasma glucose levels. (F) Liver glycogen. (G) Plasma levels for triglycerides. (H) LDL and VLDL cholesterol. (I) Plasma lactate levels. (J) Glucose oxidation was measured as the amount of ¹⁴C-labeled CO₂ release upon incubation of hearts with [U-¹⁴C] glucose. (K) Palmitate oxidation was measured from ³H₂O collected upon incubation of hearts with [9, 10-³H] palmitate. (L) Palmitate oxidation of the soleus muscle using ¹⁴C-labeled palmitate. One asterisk represents $P < 0.05$, two asterisks represent $P < 0.01$, and three asterisks represent $P < 0.001$. Number of mice (n) in each group is as indicated.

Figure 2. Txnip deficiency induces expression changes of PGC-1 α and other key metabolic genes in the liver. Mice were either in the fed or fasted (18 hour) state prior to liver RNA isolation. (A) PGC-1 α mRNA expression. (B) PEPCK mRNA expression. (C) G6Pase mRNA expression. (D) GK mRNA expression. (E) Liver protein levels of p-CREB in the fed state of WT and *Txnip*^{-/-} mice (n=4 in each group) determined by Western blot analysis. RNA was analyzed by real-time quantitative PCR and normalized against 36B4 expression. Quantitative PCR results are averages of samples run in duplicate. C3H/DiSnA were used as wild-type (WT)

The Metabolic Consequences of Txnip Deficiency

mice as indicated by solid bars, and Txnip deficient (*Txnip*^{-/-}) mice are indicated by shaded bars. One asterisk represents $P < 0.05$, two asterisks represent $P < 0.01$, and three asterisks represent $P < 0.001$. Number of mice (n) in each group is as indicated.

Figure 3. Fatty acid metabolism genes show altered expression in the liver. Mice were either in the fed or fasted (18 hour) state prior to liver RNA isolation. (A) FAS mRNA expression. (B) MCAD mRNA expression. (C) SCD1 mRNA expression. (D) AOX mRNA expression. RNA was analyzed by real-time quantitative PCR and normalized against 36B4 expression. Results are averages of samples run in duplicate. C3H/DiSnA were used as wild-type (WT) mice as indicated by solid bars, and Txnip deficient (*Txnip*^{-/-}) mice are indicated by shaded bars. One asterisk represents $P < 0.05$, two asterisks represent $P < 0.01$, and three asterisks represent $P < 0.001$. Number of mice (n) in each group is as indicated.

Figure 4. Insulin-responsive genes are not affected by Txnip deficiency. Plasma insulin and expression levels in skeletal muscle and liver in fed and fasted states. Expression levels in skeletal muscle and liver in fed and fasted states. (A) Plasma insulin levels (pg/ml). (B) Glut2 mRNA expression in the liver. (C) Glut4 mRNA expression in the skeletal muscle. Insulin levels were measured by ELISA. RNA was analyzed by real-time quantitative PCR and normalized against 36B4 expression. Results are averages of samples run in duplicate. C3H/DiSnA were used as wild-type (WT) mice as indicated by solid bars, and Txnip deficient (*Txnip*^{-/-}) mice are indicated by shaded bars. Number of mice (n) in each group is as indicated.

Figure 5. PGC-1 α and genes involved in lipid metabolism show altered expression in adipose and skeletal muscle. Mice were either fed or fasted for 18 hours prior to RNA isolation of gonadal fat pads and skeletal muscle. (A) PGC-1 α mRNA expression in adipose tissue. (B)

The Metabolic Consequences of Txnip Deficiency

FAS mRNA expression in adipose tissue. (C) Glut4 mRNA expression in adipose tissue. (D) TNF α mRNA expression in adipose tissue. (E) PGC-1 α mRNA expression in skeletal muscle. (F) AOX mRNA expression in skeletal muscle. RNA was analyzed by real-time quantitative PCR and normalized against 36B4 expression. Results are averages of samples run in duplicate. C3H/DiSnA were used as wild-type (WT) mice as indicated by solid bars, and Txnip deficient (*Txnip*^{-/-}) mice are indicated by shaded bars. One asterisk represents $P < 0.05$, two asterisks represent $P < 0.01$, and three asterisks represent $P < 0.001$. Number of mice (n) in each group is as indicated.

Figure 6. Redox state is unchanged in Txnip deficient mice. (A) Representative HPLC chromatogram of NAD⁺ and NADH in fed liver tissue (75 mg). (B) Representative HPLC chromatogram of pyrimidine dinucleotides in fasted liver tissue (75 mg). (C) NADH: NAD⁺ determined in $\mu\text{mol/g}$. Reaction of oxidized pyrimidine nucleotides with cyanide leads to two stable fluorescent products (NAD⁺-1, NAD⁺-2, NADP⁺-1, NADP⁺-2) resulting in the separation of four nucleotides in one chromatogram and the generation of six peaks in the following order: NADH, NADPH, NAD⁺-1, NADP⁺-1, NAD⁺-2, NADP⁺-2. C3H/HeJ were used as wild-type (WT) mice as indicated by solid bars, and Txnip deficient (*Txnip*^{-/-}) mice are indicated by shaded bars. One asterisk represents $P < 0.05$ and three asterisks represent $P < 0.001$. Number of mice (n) in each group is as indicated.

Figure 7. Txnip deficiency may not mediate effects through Txn. Western blot analysis of Txn and insulin reducing activity in liver. (A) Liver protein levels of Txn in *Txnip*^{-/-} and WT mice in fed and fasted states. (B) Txn activity in liver measured by insulin reducing assay in *Txnip*^{-/-} and WT mice in fed and fasted states. Reduced insulin measured at an absorbance of

The Metabolic Consequences of Txnip Deficiency

412 nm. Results are averages of samples run in duplicate. Data shown are representative of two independent experiments. C3H/DiSnA were used as wild-type (WT) mice as indicated by solid bars, and Txnip deficient (*Txnip*^{-/-}) mice are indicated by shaded bars. Number of mice (n) in each group is as indicated.

Figure 1

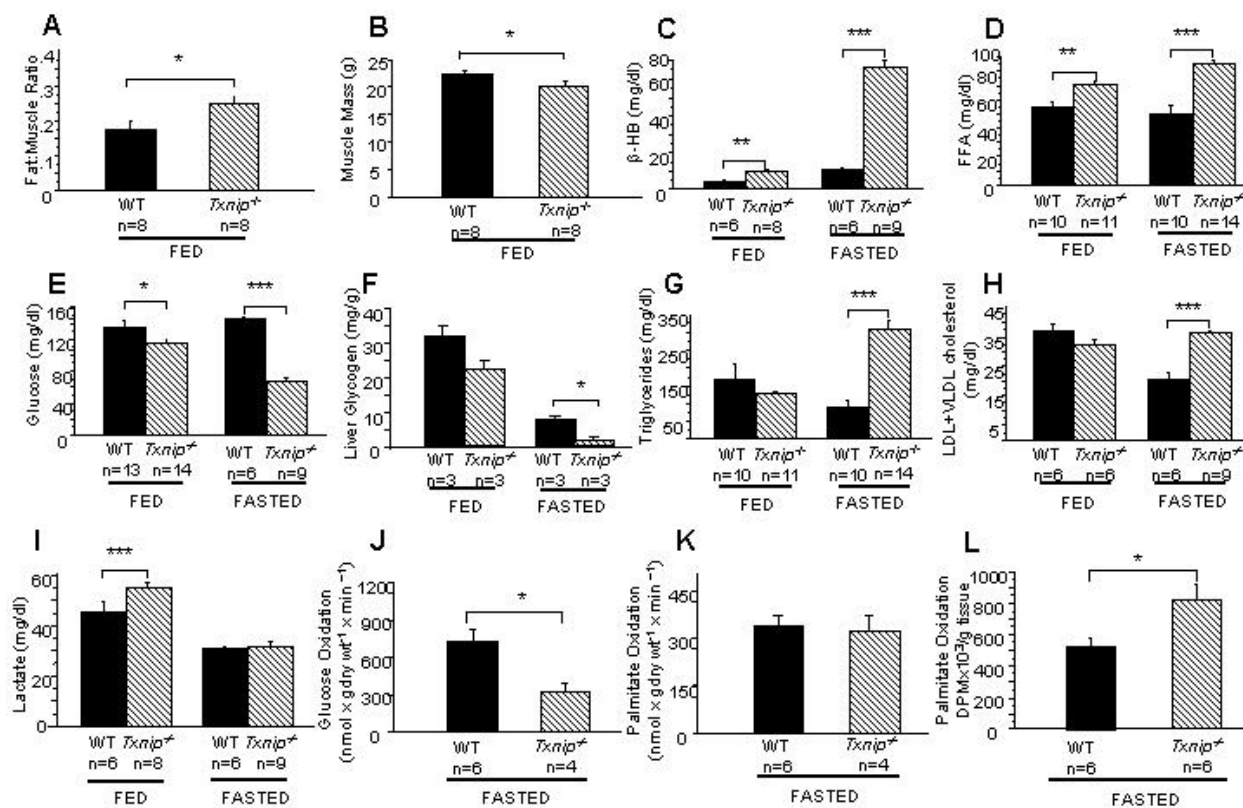


Figure 2

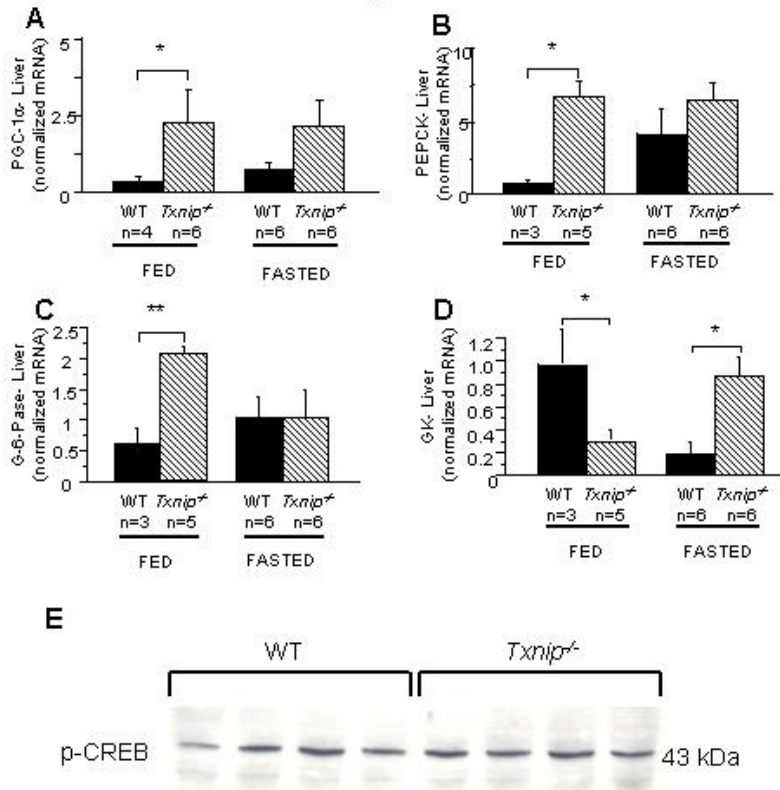


Figure 3

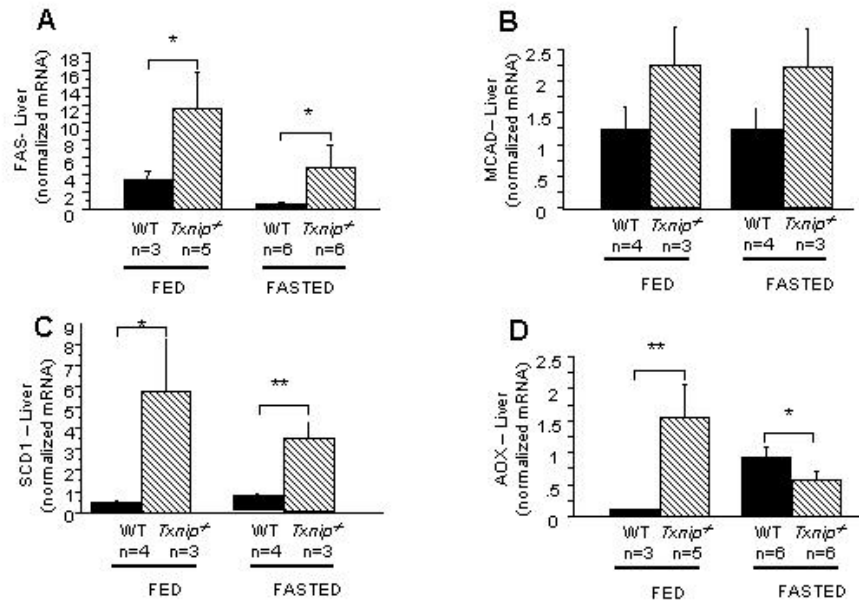


Figure 4

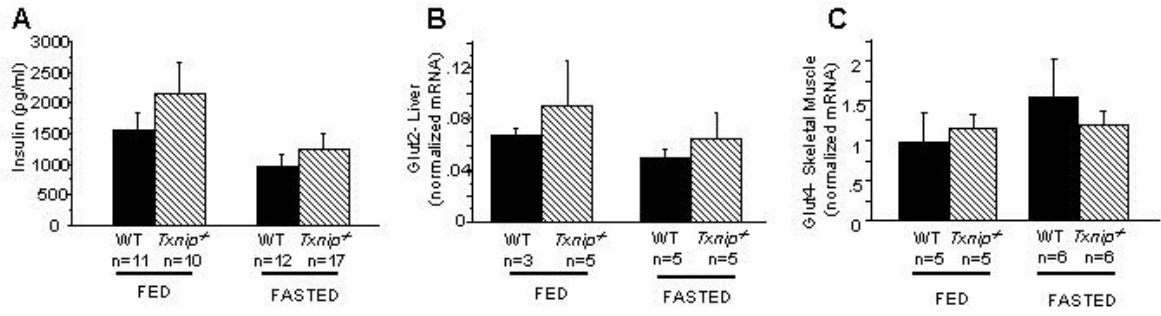


Figure 5

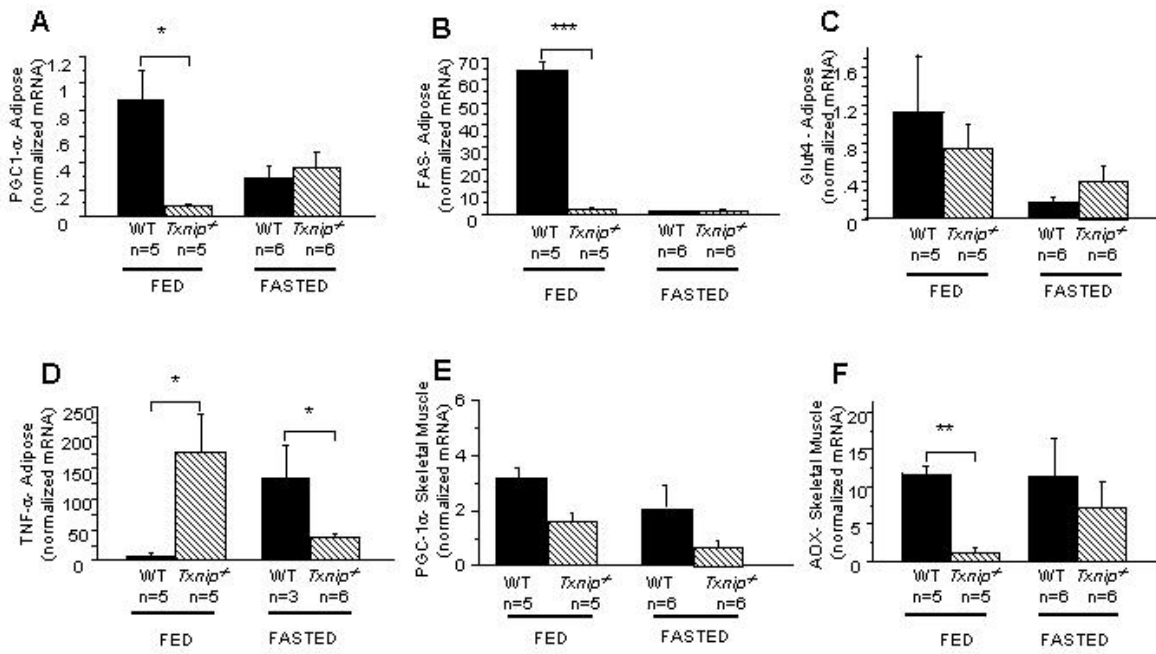


Figure 6

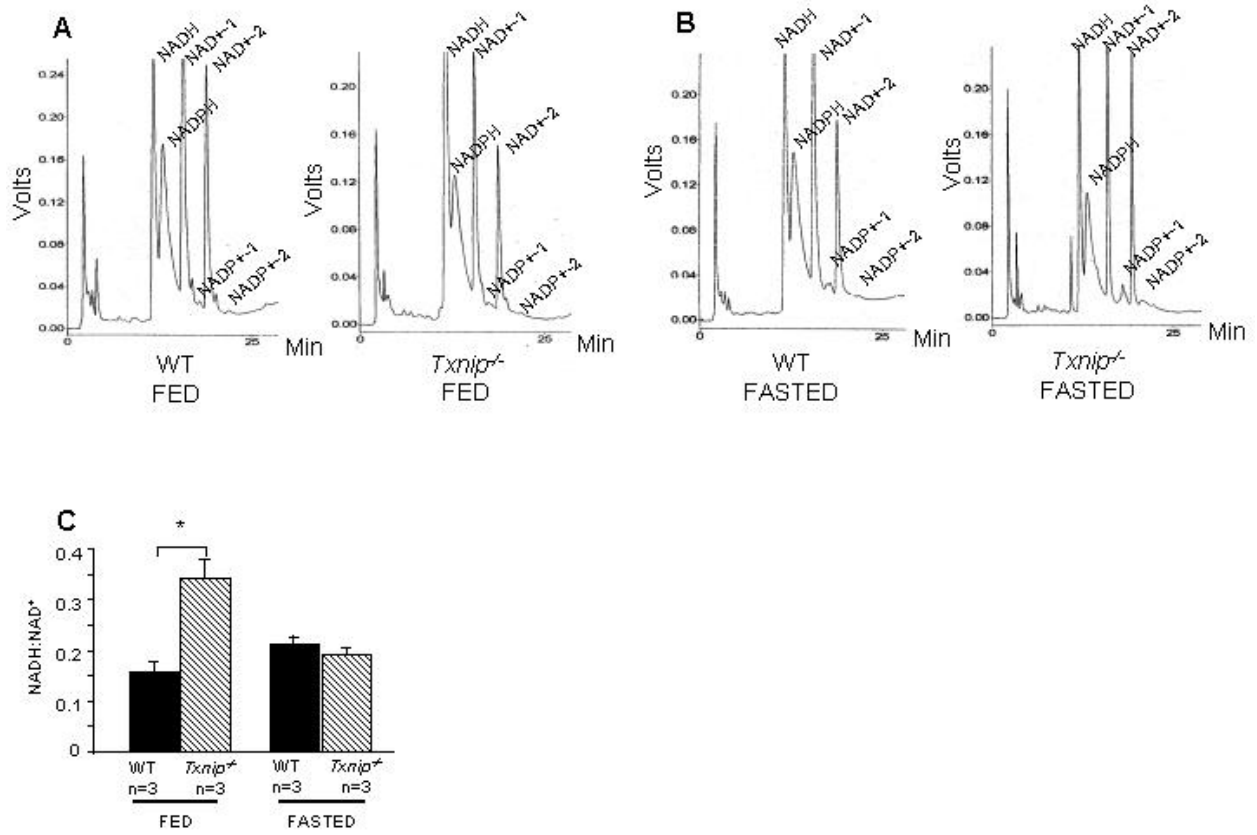


Figure 7

